2009 American Control Conference
Hyatt Regency Riverfront, St. Louis, MO, USA
June 10-12, 2009

Dynamic Modeling and System Identification of a Tubular Solid Oxide Fuel Cell (TSOFC)

Debangsu Bhattacharyya and Raghunathan Rengaswamy

Abstract— **Solid Oxide Fuel Cells (SOFCs) are high temperature fuel cells with a strong potential for stationary power house applications. However, considerable challenges are to be overcome to connect these cells to the power grid. The cells have to satisfy the changing demand of the grid without sacrificing their efficiencies and without causing any structural or material damage. Such an operation, coupled with fast and highly nonlinear transients of the transport variables, leads to a very challenging control problem. This requires an efficient and robust controller. For synthesizing such a controller, a well-validated dynamic model is essential. In this work, a dynamic model is validated by using experimental data from an industrial cell. The data are generated over a broad range of cell temperatures, reactant flow rates, DC polarizations, and amplitudes of step. In the process of validation, it is identified that the Knudsen diffusion and an extended active area for the electrochemical reactions play key roles in determining the current transients of the cell. The dynamic model is used for identification of reduced order models that can be solved in real time for implementation in the MPC framework. Several linear and nonlinear models are considered and the best model is chosen according to the AIC values of the models. Both SISO and MIMO models are identified. For the MIMO model, voltage and H_2 flow are considered as inputs. Power and utilization factors are considered as outputs. A linear model such as ARX model is found to be satisfactory for most SISO cases. However, a nonlinear model such as NAARX model with more cross terms is found to improve the model performance significantly for the MIMO case. All through this work, efforts have been made to synthesize the simplest, yet representative model that can be used for real-time applications.**

I. Introduction and Literature Review

Solid oxide fuel cells (SOFCs) are being considered for their future application in a grid-connected system. Along with other advantages, SOFCs have good load-following characteristics [1]. However, they have to follow the load in the presence of the challenging constraints without damaging the hardware of the system. An efficient controller is essential to satisfy these requirements. To synthesize such a controller, a thoroughly validated dynamic model of SOFC is critical. However, it might not be feasible to use a detailed dynamic model for real time applications. Nonetheless, the dynamic model can be utilized to identify reduced order models that can be solved in real time for online control. The detailed model can also be used for studying the transients of the system.

Most dynamic studies do not consider the detailed dynamics of the diffusion of the gaseous species through the electrodes [2], [3], [4]. Instead, a lumped term for the concentration overpotential is considered to account for the mass transfer losses inside the electrodes. The effects of the diffusive resistances on the transients of the system have been reported in the work of [5]. However, the diffusion considered in their work [5] is one dimensional and Taylor's expansion is applied to approximate the flux in the form of a transfer function. Effects of any approximation and/or assumption on the transients becomes clear if the dynamic model is validated extensively in a broad operating range. Such validation studies are rare in the existing literature. [6] have presented validation studies for a button cell in a single operating condition due to a step change in the current. However, for a well-validated dynamic model, it is essential to validate the model for steps in different inputs at various operating conditions. Besides, the magnitude and the directionality of the steps need to be varied. Presence of such a study is minimal in the open literature.

Although the detailed dynamic model is essential for control studies, it cannot be solved in real time in many circumstances. In NMPC (Nonlinear MPC) implementation, for example, it is often required to solve an optimization subproblem including the dynamic model to decide the future control moves. If a complex dynamic model is used in the optimization framework, the solution of the optimization problem in real time cannot be guaranteed. This necessitates the identification of a reduced-order model which can be used for real-time applications.

Existing literature on identification of statistical models for SOFC can be divided into two categories – Linear and Nonlinear. There are different techniques for computing the linear models such as FIR (Finite Impulse Response), ARX (Auto-Regressive with eXogeneous input), ARMAX (Auto-Regressive Moving Average with eXogeneous input), BJ (Box-Jenkins), FFT based-methods etc. Not many linear models are found in literature for identification of SOFC because of the high nonlinearity in the SOFC process. In the work of [7], a linear (ARX) model is used for identification. ANN (Artificial Neural Network) is often used to model the nonlinearity [8]. Hammerstein model structure (a static nonlinearity followed by a dynamic linear part) has been also explored [9].

In all these studies, the process model that is used to generate the data for identification is simple. The dynamic data used for identification should be representative of the system nonlinearity and, therefore, needs to be generated from a detailed model that has been validated with the experimental data over a broad operating range for steps in different inputs

D. Bhattacharyya and R. Rengaswamy are with the Department of Chemical and Biomolecular Engineering, Clarkson University, Potsdam, NY 13699-5705, USA bhattade@clarkson.edu, raghu@clarkson.edu

978-1-4244-4524-0/09/$25.00 ©2009 AACC

with varying magnitude and directionality. Most authors have validated the identified models by giving a single step in input [7], [9].

All the work mentioned above assume, *a priori*, a structure for the linear or nonlinear model and their performance are studied. A comparative performance criterion (such as Akaike Information Criterion-AIC) can be thought of as a rational approach to justify the use of a certain model structure of a given complexity. This paper addresses some of the issues mentioned above. The arrangement of the paper is as follows. In the following section, a brief account of the dynamic modeling is presented. The next section presents the validation studies of the dynamic model. The last section shows the identification of the reduced order models.

II. Modeling of SOFC

In this industrial cell, pure H_2 enters the anode gas flow channel and diffuses through the anode to the TPB (Triple Phase Boundary) for the anodic reaction. Steam gets generated due to the reaction and flows out to the flow channel. In the cathode side, air enters the channel and O_2 diffuses to the cathode TPB for the electrochemical reaction. Although, N_2 does not take part in the reaction, it may show transients until it reaches a new equilibrium. The coordinate system and the nomenclature followed in the radial and axial directions are shown in Figure 1.

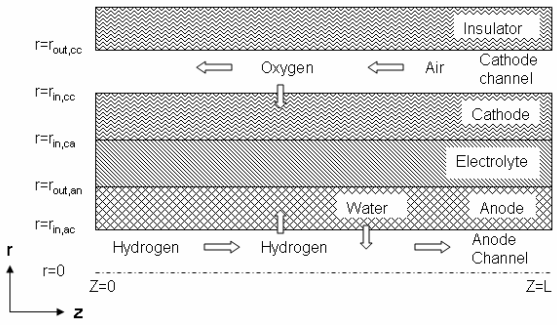

Fig. 1. Illustration of the coordinate system

The cell is divided into several segments of length $\triangle z$ by a plane perpendicular to the axial direction. In each segment, there are 5 Control Volumes(CVs): anode flow channel, anode, electrolyte, cathode and the cathode flow channel. Inside a CV, uniform transport fields are assumed. In this study, the electrolyte is considered to be solid.

A. Anode gas flow channel

1) Species Conservation: Considering the diffusion from the anode gas flow channel to the porous anode, the species conservation equations can be written as:

$$\frac{\partial C_{j,ac}}{\partial t} = -\frac{\partial}{\partial z}(C_{j,ac}u_{z,ac}) + \frac{2D_{j,eff}}{r_{in,ac}}\frac{\partial}{\partial r}(C_{j,an}) \quad (1)$$

where j denotes species H_2 and H_2O . $C_{j,ac}$ and $C_{j,an}$ are the concentrations of the species j in anode gas flow channel and inside anode respectively ($mole/m^3$). $u_{z,ac}$ is the velocity in the z direction inside the anode channel (m/s). $r_{in,ac}$ is the inside radius of the anode channel (m). $D_{j,eff}$ is the effective diffusivity of species j in electrode.

B. Cathode gas flow channel

1) Species Conservation: Because of the counter-flow configuration of the cell and the convention of the coordinate axes, the species conservation equations in the cathode flow channel can be written as:

$$\frac{\partial C_{j,cc}}{\partial t} = \frac{\partial}{\partial z}(C_{j,cc}u_{z,cc}) - \frac{2D_{j,eff}r_{in,cc}}{r_{out,cc}^2 - r_{in,cc}^2}\frac{\partial}{\partial r}(C_{j,ca}) \quad (2)$$

where j denotes species O_2 and N_2 . $r_{in,cc}$ and $r_{out,cc}$ are inside and outside radius (m) of the cathode channel respectively. $C_{j,cc}$ and $C_{j,ca}$ are the concentrations of the species j in cathode gas flow channel and inside cathode respectively ($mole/m^3$). $u_{z,cc}$ is the velocity inside the cathode channel (m/s) in the z direction.

C. Anode

Hydrogen gets consumed due to the reaction at the TPB while steam is generated. Considering the velocity to be zero in the porous region, the species conservation equation can be written as [10]:

$$\varepsilon_{an}\frac{\partial C_{j,an}}{\partial t} = D_{j,eff}(\frac{1}{r}\frac{\partial}{\partial r}(r\frac{\partial C_{j,an}}{\partial r}) + \frac{\partial^2 C_{j,an}}{\partial z^2}) \quad (3)$$

Here j denotes species H_2 and H_2O and ε_{an} is the porosity of the anode.

D. Cathode

As in the anode, the species conservation equations can be written as :

$$\varepsilon_{ca}\frac{\partial C_{j,ca}}{\partial t} = D_{j,eff}(\frac{1}{r}\frac{\partial}{\partial r}(r\frac{\partial C_{j,ca}}{\partial r}) + \frac{\partial^2 C_{j,ca}}{\partial z^2}) \quad (4)$$

Here j denotes species O_2 and N_2 and ε_{ca} is the porosity of the cathode.

The effective diffusion coefficient of species j is expressed by Bosanquet equation [11]. The detailed calculation of the diffusion coefficients are shown in [12].

E. Electrochemical Reaction:

Nernst potential is given by :

$$E_{Nernst} = \frac{-\triangle G^0}{2F} + \frac{R_u T}{2F}\ln(\frac{P_{H_2}P_{O_2}^{0.5}}{P_{H_2O}}) \quad (5)$$

where $\triangle G^0$ is the change in standard state Gibbs' free energy of oxidation reaction of hydrogen, T is the temperature of PEN, P_{H_2} and P_{H_2O} are the ratios of partial pressures of hydrogen and water respectively at the anode TPB over the standard atmospheric pressure, P_{O_2} is the partial pressure of oxygen at the cathode TPB over standard atmospheric pressure and R_u is the universal gas constant.

The ohmic losses in the electrodes and the electrolyte are assumed to follow Ohm's law. The calculation of the ohmic resistances and the temperature-dependent relations used can be found in [12]. For calculating the activation polarization at

the electrodes, the hyperbolic sine approximation of Butler-Volmer equation is considered. The exchange current densities in the electrodes are considered to be temperature and concentration dependent.

Initially, only binary diffusivity was considered for the species transport. The simulation results showed a much lower overshoot in the current than observed in the experimental data. The time constant and the settling time in the simulation results were lower than the experimental data too. Observing the mismatch with the experimental data, Knudsen diffusion is considered in the next level of model. Although, the overshoot, time constant, and the settling time matched quite well with the experimental data, the steady state current in the simulation results fell much lower than the experimental data. Because of this mismatch, an extended active area for the electrochemical reactions have been considered. A number of authors have reported the existence of an extended TPB length and surface area for the electrochemical reactions [13], [14], [15]. In this work, the extended area for reactions have been characterized as regularly spaced cylinders. This is illustrated in Figure 2. In Figure 2, 'c' is the radius of the cylinder and '$2x$' is the periodic spacing of the cylinders. 'c' is a measure of the grain size of the electrolyte particles in the electrode. 'h' is the height of a cylinder. In order to reduce the number of tuning parameters and simplicity, 'h' is considered to be same for both the electrodes. Assuming uniform porosity in the active area, 'x' can be expressed in terms of 'c' and the porosity. Therefore 'h' is the only tuning parameter in the calculation of the active area. The gradual development of the detailed dynamic model can be found in [16].

III. Validation Studies

A. Data for Validation

The industrial cell studied here is a counter-current anode-supported tubular solid oxide fuel cell. The cell is well-insulated and kept inside a furnace that maintains the temperature of the cell with a feedback control. As a result, under most operating conditions, the cell considered can be assumed to be isothermal. The cell is started up and the temperature is slowly brought to 700^oC. After the Open Circuit Potential (OCP) of the cell stabilizes at this temperature, data collection is started. First, the steady state data of the cell are collected at various temperatures and flowrates of H_2. The dynamic data are collected by stepping up and down the cell voltage at various temperatures and different H_2 flowrates. After that, the dynamic data are collected by introducing steps of different magnitude and directionality in the flowrate of H_2. The voltage and current data are collected by a Tektronix TDS 3014B oscilloscope. The sampling time is 0.1 ms and the data are collected for 1 s. This sampling time is found to be adequate to capture the current transients as well as the entire range of data until the cell reaches the steady state.

B. Processing of Data

The experimental data of current, voltage and flow are very noisy. Since the voltage and flow are inputs to the model, clean data for these two inputs are required to perform model validation. The voltage data are first filtered by implementing a 3^{rd} order butterworth filter with a normalized cut-off frequency of 0.1. In the case of a step down in voltage, the input voltage data could be curve fit by considering a step fall followed by a transient like a first order system. For the step up in voltage, the transient in the input voltage can be fit only by a first order transfer function. Flow data are found to be extremely noisy. Because of the overlapping of the signal and noise frequency, the data could not be cleaned properly so as to show any clear trend. However, it is observed that the step in the input flow can be approximated by a second order transfer function having a damping ratio (ζ) of 0.9 , DC gain (G_{dc}) of 1.0 and time constant (τ) of 0.78. These values are found out by manipulating the input data for flow at 850^oC, 0.65 V and for flow steps of 40 ml/min to 45 ml/min H_2 flowrate. The characteristic parameters are manipulated such that the simulation results have minimal error with the experimental data in a least squares sense. The same parameters are used to find the input data for all other steps in flow.

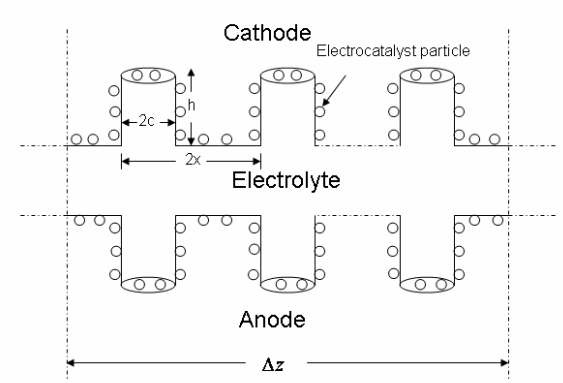

Fig. 2. A model of the active reaction zone

C. Steady State Model Validation

Both the steady state and the dynamic results reported hereafter are based on the cylindrical characterization of the active area. The steady state model is validated with the data at 700^oC, 800^oC and 850^oC. At each temperature, the model validation is done for both 35 ml/min and 45 ml/min of H_2 flowrates. Figure 3 is an example of the validation at 700^oC and 35 ml/min H_2 flowrate. Figure 3 shows a very good match between the simulation results and the experimental data over the whole range of the DC potentials.

D. Dynamic Model Validation for Steps in Voltage

The voltage signal is pre-processed and used as an input voltage to the dynamic model. The step in voltage from

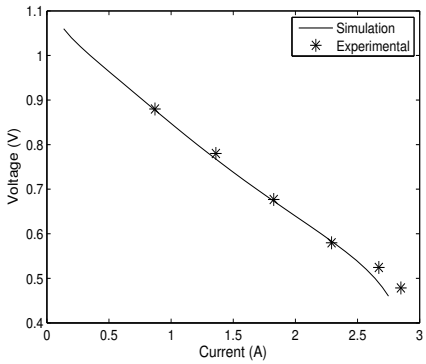

Fig. 3. Steady state model validation at 700^oC and 35 ml/min H_2 flowrate

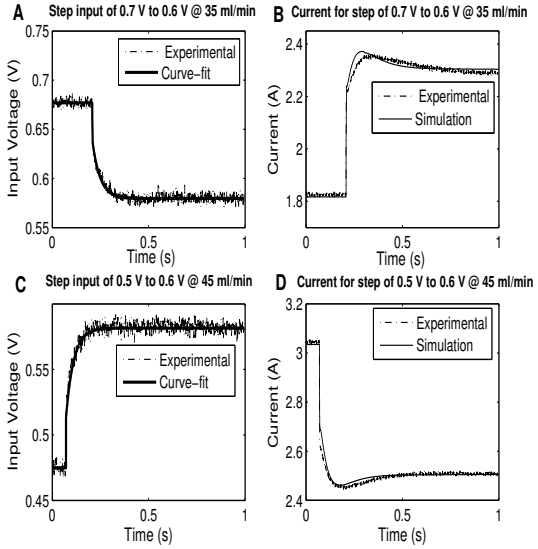

Fig. 4. Input voltages and the current transient for steps in voltages at 700^oC

0.7 V to 0.6 V given at 700^oC and 35 ml/min is shown in Figure 4 A. The curve-fit signal matches the input data very well. Figure 4B shows that the transients are well predicted by the model. The experimental data for current transients shown here and in other figures later in this work are filtered through a 3^{rd} order butterworth filter. Figure 4C is the actual signal for voltage step from 0.5 V to 0.6 V given at 700^oC and 45 ml/min. Figure 4D shows that the simulation results capture the nature of the experimental data.

The validation of the dynamic model is done at other temperatures and flowrates of H_2 for steps in voltage. The fit of the dynamic model is found to be satisfactory for all the experimental data.

E. Dynamic Model Validation for Steps in Hydrogen Flow

Figure 5 shows an example of the model validation for steps in H_2 flow. The input flow signal is plotted with respect to the right axis. The simulation values and the experimental data, plotted with respect to the left axis, are found to match well. Similar kind of fit is obtained for all other steps in H_2 flow.

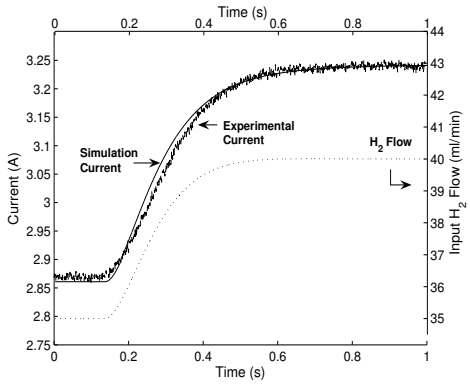

Fig. 5. Comparison of results for H_2 flow stepping from 35 ml/min to 40 ml/min

IV. Identification Study

A. Models of Different Forms

In this work, we have considered Linear in Parameter (LIP) models. The parameter vector is estimated by the method of least squares. The simplest dynamic model considered here is the Finite Impulse response (FIR) model [17]. The other form of linear model considered is the ARX model. NAARX (Nonlinear Additive Auto-Regressive with eXogenous inputs) models are considered as one of the forms for the nonlinear models. NAARX models can be expressed by:

$$y(k) = \sum_{i=0}^{n} f_i(u(k-i)) + \sum_{j=1}^{r} s_j(y(k-j)) \qquad (6)$$

where f_i and s_j are nonlinear functions. In this study, f and s are represented by a polynomial of order P and Q respectively. A second order Volterra model is considered as another nonlinear model. It is given by [18]:

$$y(k) = \sum_{i=0}^{M} h_1(i)u(k-i) + \sum_{i=0}^{M}\sum_{j=0}^{M} h_2(i,j)u(k-i)u(k-j) \qquad (7)$$

In this work, a modified Wiener model structure has also been explored for SOFC identification. In this structure, the input sequence $u(k)$ is transformed to an intermediate sequence $\phi(k)$ by a linear ARX model. Then $\phi(k)$is transformed to the final output $y(k)$ by the Volterra model. Unlike a typical Wiener model, the nonlinear block has memory in this modified structure.

B. Model Selection Criteria

In the presence of different competing models, several information-theoretic criteria have been proposed such as Final Prediction Error (FPE), Akaike Information Criterion

(AIC) [19], Minimum Description Length (MDL) Criterion [20] etc. However, in this work, AIC has been used as it is one of the well-accepted and tested criterion for selecting statistical models. Model complexity of a given form is increased until the AIC value changes significantly. If there is no significant difference in the AIC values between two models, then the simpler model is chosen. Root Mean Square Error (RMSE) of all the models are also compared for observing the change in the prediction error with an increase in the model complexity.

C. SISO Model

For the SISO model, the cell terminal voltage is considered as the input and cell power is considered as the output. The performance of the input-output model is observed to be very poor and does not improve any significantly when more terms are included in the model.

Figure 6 shows the performance of the ARX model and the modified Wiener system. Although not clear from the figure, the performance of the modified Wiener system is marginally better than that of the ARX model. Two forms of

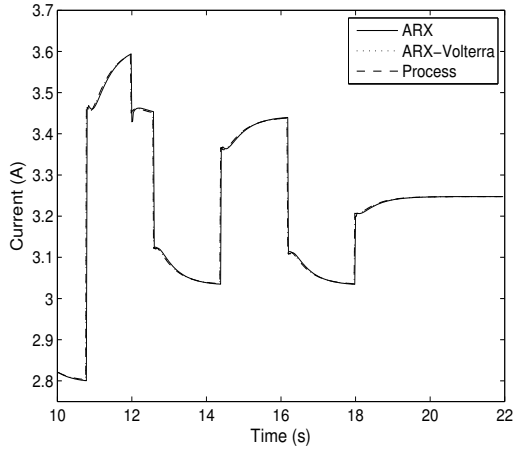

Fig. 6. Performance of ARX model and ARX model followed by Volterra model

the NAARX models are considered in the identification of the SISO model. One form considers the cross terms between the inputs. The other form does not consider any cross term. Performances of both the NAARX models are better than that of the ARX model. The performance of the modified Wiener system is marginally better than that of the NAARX models. But in view of the simplicity of the model, the ARX model is chosen as the best SISO model for this cell and for this input-output pair.

D. MIMO Model

In the MIMO model, a two input/output system is studied. The inputs are cell voltage and the flowrate of H_2. The outputs are power and utilization factor (UF) of H_2. For identification of the MIMO model, steps in both the inputs are introduced simultaneously. The performances of both the input-output model and the ARX model are not good. The modified Wiener system is finally discarded because of its complexity. Four forms of the NAARX model are considered. In model 1, no cross-terms between the inputs are considered. In model 2, only self-cross terms (such as $u_1(k)u_1(k-1)$) are considered along with all the terms used in model 1. In model 3, cross-terms between the inputs corresponding to the same time instant (such as $u_1(k)u_2(k)$) are considered along with the terms used in model 2. In model 4, all possible combinations of cross-terms between the inputs based on the polynomial order are considered. The number of terms in each model is increased until significant changes in AIC and RMSE values are observed. Figure 7A shows the fit of each model for the transients in power. Performance of model 1 is very poor. The goodness of fit improves significantly as cross-terms are introduced in model 2. Performance of model 2 is shown in Figure 7B. As more cross-terms are considered, model performance improves as seen in Figure 7C. Based on the AIC values, model 3 is the final model for power. Figure 7D shows the error profiles as model complexity is increased. It is observed that the error corresponding to model 3 is very close to zero.

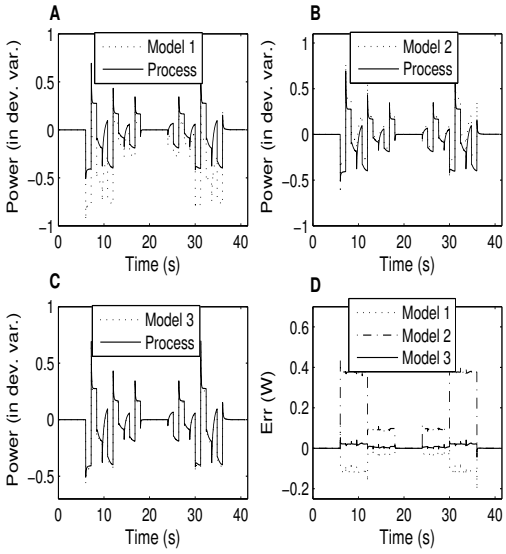

Fig. 7. Performance of different models for power corresponding to simultaneous step in voltage and H_2 flow

For the transients in UF , model 4 is the final model based on the AIC values. The AIC and RMSE values for the identification of the model for UF are reported in Table I.

TABLE I
AIC AND RMSE VALUES FOR MIMO MODELS FOR UF

	Model 1	Model 2	Model 3	Model 4
AIC	$+1.1 \times 10^3$	-5.2×10^3	-8.0×10^3	-1.43×10^4
RMSE	4.9625	0.0645	0.0380	0.0132

V. Conclusions

In this paper, a dynamic model of an anode-supported tubular counter-flow SOFC is validated with the experimental data. In the process of validation, it is observed that the mass transfer resistances inside the electrodes play a key role in determining the transients of the system. The effects of the Knudsen diffusion and an extended active area for the electrochemical reactions are considered based on the mismatch between the experimental data and the simulation results. A cylindrical characterization of the active area is found to be adequate for model validation.

Reduced order SISO and a MIMO models are identified using the detailed first principles model. The modified Wiener system performs very well for all the simulated cases. However, it is not selected as the final model in view of the complexities associated with it for implementation in a MPC framework and for execution of the block in real time. For the voltage-power SISO model, ARX model is chosen as the final model. In the identification of the MIMO model, the model performance is found to improve as more cross-terms are considered.

References

[1] E. Achenbach, "Response of a solid oxide fuel cell to load change," *Journal of Power Sources*, vol. 57, pp. 105–109, 1995.

[2] J. Padullés, G. Ault, and J. McDonald, "An integrated sofc plant dynamic model for power systems simulation," *Journal of Power Sources*, vol. 86, pp. 495–500, 2000.

[3] N. Lu, Q. Li, X. Sun, and M. A. Khaleel, "The modeling of a standalone solid-oxide fuel cell auxiliary power unit," *Journal of Power Sources*, vol. 161, pp. 938–948, 2006.

[4] A. M. Murshed, B. Huang, and K. Nandakumar, "Control relevant modeling of planer solid oxide fuel cell system," *Journal of Power Sources*, vol. 163, pp. 830–845, 2007.

[5] Y. Qi, B. Huang, and J. Luo, "Dynamic modeling of a finite volume of solid oxide fuel cell: The effect of transport dynamics," *Chemical Engineering Science*, vol. 61, pp. 6057–6076, 2006.

[6] R. S. Gemmen and C. D. Johnson, "Effect of load transients on sofc operation-current reversal on loss of load," *Journal of Power Sources*, vol. 144, pp. 152–164, 2005.

[7] F. Jurado, "Modeling sofc plants on the distribution system using identification algorithm," *Journal of Power Sources*, vol. 129, pp. 205–215, 2004.

[8] J. Arriagada, P. Olausson, and A. Selimovic, "Artificial neural network simulator for sofc performance prediction," *Journal of Power Sources*, vol. 112, pp. 54–60, 2002.

[9] F. Jurado, "A method for the identification of solid oxide fuel cells using a hammerstein model," *Journal of Power Sources*, vol. 154, pp. 145–152, 2006.

[10] R. B. Bird, W. E. Stewart, and E. N. Lightfoot, *Transport Phenomen, Second Edition*. New York,USA: John Wiley & Sons,Inc., 2002.

[11] A. L. Hines and R. N. Maddox, *Mass Transfer:Fundamentals and applications*. Englewood Cliffs,NJ,USA: Prentice Hall, 1985.

[12] D. Bhattacharyya, R. Rengaswamy, and F. Caine, "Isothermal models for anode-supported tubular solid oxide fuel cells," *Chemical Engineering Science*, vol. 62, pp. 4250–4267, 2007.

[13] C. W. Tanner, K.-Z. Fung, and A. V. Virkar, "The effect of porous composite electrode structure on solid oxide fuel cell performance:i. theoretical analysis," *Journal of The Electrochemical Society*, vol. 144(1), pp. 21–30, 1997.

[14] M. Mogensen, K. V. Jensen, J. M. Juhl, and P. Søren, "Progress in understanding sofc electrodes," *Solid State Ionics*, vol. 150, pp. 123–129, 2002.

[15] M. Brown, S. Primdahl, and M. Mogensen, "Structure/performance relations for ni/yttria-stabilized zirconia anodes for solid oxide fuel cells," *Journal of The Electrochemical Society*, vol. 147(2), pp. 475–485, 2000.

[16] D. Bhattacharyya, R. Rengaswamy, and F. Caine, "Transient and diagnostic studies of a tubular sofc using a dynamic model," *Being submitted to Chemical Engineering Science*.

[17] L. Ljung, *System Identification:Theory for the user, Second ed.* Upper Saddle River,NJ,U.S.A.: Prentice Hall PTR, 1999.

[18] F. J. Doyle III, R. K. Pearson, and B. A. Ogunnaike, *Identification and control using Volterra models*. London,U.K.: Springer, 2002.

[19] H. Akaike, "A new look at the statistical model identification," *IEEE Trans. on Automatic Control*, vol. 19, pp. 716–723, 1974.

[20] G. Liang, D. M. Wilkes, and J. A. Cadzow, "Arma model order estimation based on the eigenvalues of the covariance matrix," *IEEE Trans. on Signal Processing*, vol. 41(10), pp. 3003–3009, 1993.